

Thermal properties of modified banana trunk fibers

Kathiresan Sathasivam ·
Mas Rosemal Hakim Mas Haris

Received: 15 July 2010 / Accepted: 8 July 2011 / Published online: 24 July 2011
© Akadémiai Kiadó, Budapest, Hungary 2011

Abstract Thermal decomposition of an agrowaste, namely banana trunk fibers (BTF) were investigated by thermogravimetry (TG) and derivative thermogravimetry (DTG) up to 900 °C at different heating rates (from 5 to 100 °C/min). The BTF was subjected to modification by means of various known chemical methods (mercerization, acetylation, peroxide treatment, esterification, and sulfuric acid treatment). Various degradation models, such as the Kissinger, Friedman, and Flynn–Wall–Ozawa were used to determine the apparent activation energy. The obtained apparent activation energy values (149–210 kJ/mol) allow in developing a simplified approach to understand the thermal decomposition behavior of natural fibers as a function of polymer composite processing.

Keywords Apparent activation energy · Degradation models · Thermal decomposition · Modified fiber · Polymer composite

Introduction

In recent years, the use of natural fibers as reinforcement or filler in the manufacture of fiber thermoplastic composites has been of great interest to many researchers [1]. These fibers have many advantages, such as high specific

strength, cost density, renewability, recyclability, abrasiveness, and biodegradability properties [2–4]. Natural fibers could replace synthetic fibers in many applications, where cost outweighs high composite performance requirements [5]. However, the leading disadvantages of natural fibers in composites are their susceptibility to moisture uptake [6–8], incompatibility between hydrophilic natural fibers and hydrophobic polymers [9], low thermal resistance, and inconsistency in quality [10]. To improve the compatibility of the two phases in such composites, chemical modifications are often carried out to optimize the interface of fibers [11]. By introducing chemical modification, the hydroxyl groups are activated, or new moieties are introduced that can effectively interlock with the matrix [12]. Chemical modifications of natural fibers aimed at improving the adhesion with a polymer matrix were investigated by a number of researchers [13–15]. During composite processing, natural fibers are usually subjected to thermal degradation [16]. With this in view, the knowledge and understanding of thermal decomposition process of natural fibers are vital to aid in better composite processing, thus producing thermally stable composite.

Lignocellulosic natural fibers have been studied by many researchers and proved to be good reinforcements in thermoset and thermoplastic matrices [17]. Thus, extensive researches have been carried out to understand the individual behaviors of the main components of natural fibers (cellulose, lignin, and hemicelluloses) [18]. In the literature, there are several attempts to characterize banana trunk fibers (BTF). Table 1 depicts the reported chemical composition on BTF [18–20]. The tensile properties of BTF as determined by Nolasco et al. 1998 [20] and Satyanarayana and Wypych 2007 [21] are as follows: Young Modulus (27–32 GPa), Tensile strength (700–800 MPa), and

K. Sathasivam (✉)
Department of Materials Science, Faculty of Applied Sciences,
AIMST University, Jalan Bedong-Semeling, 08100 Bedong,
Kedah Darul Aman, Malaysia
e-mail: skresan_jps@yahoo.com

M. R. H. M. Haris
School of Chemical Sciences, Universiti Sains Malaysia,
11800 Minden, Penang, Malaysia

Table 1 Reported chemical composition of BTF

Variety	Moisture/%	Ash/%	Holocellulose/%	Cellulose/%	Hemicellulose/%	Lignin/%	Extractives/%	Crystallinity/%	Reference
<i>Musa sapientum</i>	8.57 ± 0.19	4.14 ± 0.92	50.92 ± 0.34	50.15 ± 1.09	0.77 ± 0.58	17.44 ± 0.19	–	39	[18]
<i>Musa acuminata</i>	9.74 ± 1.42	8.65 ± 0.10	–	31.27 ± 3.61	14.98 ± 2.03	15.07 ± 0.66	4.46 ± 0.11	–	[19]
<i>Musa cavendish</i>	10–12	1–2	66–73	60–65	6–8	5–10	–	–	[20]

elongation (2.5–3.7%). The mechanical properties of banana fibers such as functions of the fiber diameter, test length, and speed of testing were studied by Kulkarni et al. [22] and reported that initial modulus, ultimate tensile strength and % of elongation have insignificant variations in their fibers of diameter ranging from 50 to 250 μm . However, the ultimate tensile strength and breaking strain was found to decreased as the fiber length increased.

Idicula et al. [23] reported that user-friendly and cost-effective composite materials possessing appropriate stiffness and damping behavior can be obtained by hybridising banana and sisal fibers. The role of fiber/matrix interactions of chemically modified banana fiber/polyester composites was studied by Pothan et al. [24], and concluded that the chemical modification improves the storage modulus of these composites. Sapuan et al. [25] developed composite-woven banana fiber reinforced epoxy composites for household utilities. Kalia et al. [26] reported that banana fiber reinforced polyester composites were found to be dependent on the fiber content and the fiber surface modification.

This study aims to investigate the thermal decomposition of modified banana stem fibers using the thermogravimetric analysis (TG) technique. Kissinger [27], Friedman [28], and Flynn–Wall–Ozawa [29, 30] equations were employed to determine the activation energy of the thermal decomposition reaction.

Theoretical approach for thermal analysis

All kinetics equations are generally described as,

$$\frac{d\alpha}{dt} = kf(\alpha), \quad (1)$$

wherein k is the rate constant and $f(\alpha)$ is the reaction model, a function depending on the actual reaction mechanism. Equation 1 expresses the rate of conversion of α , $\frac{d\alpha}{dt}$ at a constant temperature as a function of the reactant concentration loss and rate constant. The conversion rate, α , is defined as:

$$\alpha = \frac{W_o - W_t}{W_o - W_f}, \quad (2)$$

wherein W_o , W_t , and W_f are the initial weight, weight at time t , and final weight, respectively. The rate constant, k is deduced using the Arrhenius equation:

$$k = Ae^{-E_a/RT}, \quad (3)$$

wherein E_a is the activation energy, R is the gas constant (8.3145 J/K/mol), A is the pre-exponential factor (/min), and T is the absolute temperature in Kelvin (K). By combining Eqs. 2 and 3, the following relationship is derived:

Table 2 Methods for calculating kinetic parameters using TGA data

Method	Expression	Plots	Reference
Kissinger	$-\ln(\beta/T_m^2) = E_d/RT_m - \ln(AR/E_d)$	$\ln(\beta/T_m^2)$ against $1/T_m$	[27]
Friedman	$\ln(dx/dt) = \ln(Z) + n \ln(1 - \alpha) - E_a/RT$	$\ln(dx/dt)$ against $1/T$	[28]
Flynn–Wall–Ozawa	$\log \beta = \log(AE_a/Rg(\alpha)) - 2.315 - 0.4567E_a/RT$	$\log \beta$ against $1/T$	[29, 30]

$$\frac{d\alpha}{dt} = Ae^{-E_a/RT}f(\alpha) \quad (4)$$

By introducing the heating rate, $\beta = \frac{dT}{dt}$, into Eq. 4, Eq. 5 is obtained:

$$\frac{d\alpha}{dT} = \left(\frac{A}{\beta}\right)e^{-E_a/RT}f(\alpha) \quad (5)$$

Table 2 is a summary of the common “free-model” methods used in this study. In the Kissinger method, $\ln(\beta/T_m^2)$ is plotted against $1/T_m^2$ for a series of experiments at different heating rates with the peak temperature, T_m , obtained from the DTG curve. In the Friedman method, the kinetics parameters, such as activation energy E_a , order n , and frequency factor Z was determined by using the relationship between the weight-loss rate, $\ln(dx/dt)$ and $1/T$, where α is the fractional weight loss. The iso-conversional Flynn–Wall–Ozawa (F–W–O) method is the integral method, which leads to $-E_a/R$ from the slope by plotting $\log \beta$ against $1/T$ at any certain conversion rate.

Experimental

Materials

Banana trunks from the family of *Musa acuminata* × *balbisiana* Colla (ABB Group) cv ‘Pisang Awak’ were collected in Sungai Petani, Kedah, Malaysia. The trunks were chopped into cubes of average size of 2 × 2 cm. The cubes were boiled in distilled water for 1 h and then dried in an oven at 70 °C until a constant mass was obtained. The resulting material was grounded using a Waring Commercial high speed blender and sieved to obtain BTF of the size 212–350 microns. Surface area of the fibers was characterized according to the method described by Horsfall and Spiff [31], and was found to be 28.75 ± 1.57 m²/g.

Treatments of BTF

The BTF were modified according to the methods reported in the literature: (i) mercerization (BTF-1), the fibers were immersed in 5% NaOH solution for 48 h at

25 °C [32], (ii) acetylation (BTF-2), the mercerized fibers were soaked in glacial acetic acid for 1 h, separated by decantation and then soaked in acetic anhydride containing 2 drops of concentrated H₂SO₄ for 2 min [32], (iii) peroxide treatment (BTF-3), the mercerized fibers (30 g) were immersed in 1 L of a 6% solution of benzoyl peroxide in acetone for 30 min [33], (iv) stearic acid treatment (BTF-4), a mixture containing 1.0 g of the fibers, 0.2 g of stearic acid, and 2 drops of concentrated H₂SO₄ in 100 mL of *n*-hexane was refluxed in a Dean–Stark apparatus at 65 °C for 6 h [34], and (v) sulfuric acid treatment (BTF-5), 1:1 mass ratio of the fibers along with concentrated H₂SO₄ was heated in a muffle furnace for 24 h at 150 °C [35]. All resulting fibers were washed with ample amount of water till a pH close to neutral was obtained. As for comparison, the untreated BTF are designated as UMBTF.

Thermogravimetry

Thermogravimetric analyses (TG) were performed using Perkin-Elmer Thermograph (model TGA 7) with mass of samples 10 ± 1 mg. The analyses were run under a stream of nitrogen (60 mL/min) at six different heating rates of 5, 10, 20, 50, 75, and 100 °C/min within 50–900 °C. Before each run, the furnace was purged with nitrogen for 20–30 min to prevent any unwanted oxidative decomposition.

Results and discussion

UMBTF

It is a common fact that the major components of lignocellulosic fibers are hemicellulose, cellulose, and lignin. According to Yang et al. [36], the main thermal decomposition of lignocellulosic materials generally occur over the temperature range of 200–400 °C. Hemicelluloses, being the light fraction component decompose at the low temperature region between 220 and 315 °C. Cellulose is the last component to decompose at the high temperature range of 315–400 °C. Among the three components, lignin was the most difficult component to decompose. The

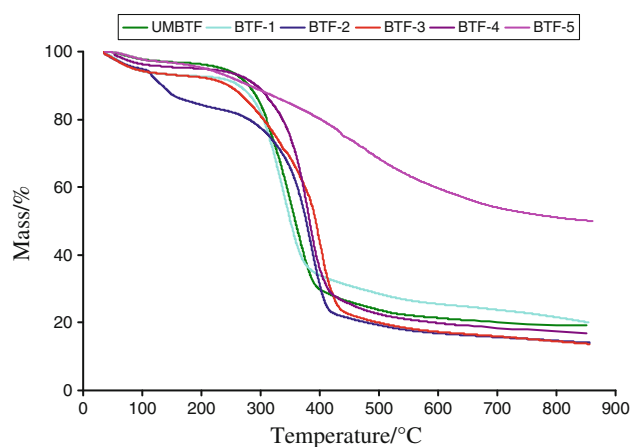


Fig. 1 Thermogravimetric decomposition process of the fibers at a heating rate of 20 °C/min

degradation of lignin is represented by the high temperature “tails” shown in all curves in Fig. 1.

Its decomposition happens slowly under the whole temperature ranges from ambient to 900 °C as shown in Fig. 1a.

Figure 1b shows the derivative thermogravimetry (DTG) of UMBTF under nitrogen. An obvious “shoulder peak” is observed, which was normally considered as the result of thermal decomposition of hemicelluloses in an inert atmosphere [37]. However, these shoulder peaks are not obvious in certain cases as the low temperature hemicelluloses bands are overlapped with the main cellulose peaks. The presence of the three major peaks in the DTG curve may be qualitatively explained as follows. The DTG curve of the untreated banana fibers shows an initial peak between 30 and 134 °C, [38] which corresponds to a mass loss of absorbed moisture with approximately 7%. The second peak at 134–238 °C could be generated by the decomposition of hemicelluloses, and the major peak with a maximum decomposition temperature at 302 °C is probably attributed to cellulose decomposition. The mass loss from 238 to 900 °C is about 65% which is probably due to the loss of cellulose and lignin. The char residue at 900 °C is 17%.

The higher activity of hemicellulose in thermal decomposition might be attributed to its chemical structure. Hemicellulose has a random amorphous structure with little strength, and it is easily hydrolyzed by dilute acid or base. In contrast, the cellulose molecule is a very long polymer of glucose units without any branches, and it is crystalline, strong, and resistant to hydrolysis. Lignin is different from cellulose and hemicelluloses, which are composed of polysaccharides, because it is composed of three kinds of benzene-propane and is heavily cross-linked [39]. The thermal stability of lignin is very high, thus making it difficult to decompose.

Modified fibers

Thermogravimetry (TG) and derivative thermogravimetry (DTG) curves of modified BTF fibers are shown in Fig. 1 and the data are summarized in Table 3. An increase in the degradation temperature was observed in BTF-1, BTF-2, and BTF 3. This was due to the removal of more non-cellulosic material; hence, the high degree of structural order was retained. This revealed a relationship between the structure and the thermal degradation of cellulose. A greater crystalline structure required a higher degradation temperature [40]. However, both the non-cellulosic components and the crystalline order of cellulose played an important role in the thermal degradation of the fibers. Mercerization disrupts the hydrogen bonding in the network structure, and thus increases the surface roughness. This treatment removes a certain amount of lignin, wax, and oils from the external surface of the fiber cell wall, depolymerizes cellulose, and exposes the short length crystallites. Acetylation also removes waxy layer from the fiber surface. Peroxide treatment was found to leach out of the waxes, gums, and pectic substances, and hence causes fibrillation. In the case of BTF-4, the decomposition temperature was 278 °C. The thermal stability of cellulose fibers is affected by the crystalline order, which decreases after substitution of cellulose hydroxyls with organic acids [41]. Thus, the thermal stability of cellulose esters is lower than that of original cellulose. The treatment with sulfuric acid significantly modifies the TG and DTG curves of BTF-5 (Figs. 1, 2b). The carbonaceous residue was found to be 50%. The mass loss occurs in a single wide step and the characteristic peak of maximum rate of mass loss cannot be easily distinguished. This agrees well with the findings of Alvarez et al. [42]. These results suggest that the sulfuric acid, an efficient dehydration agent [43], causes the removal of the hemicellulosic fraction (the lightest components of the lignocellulosic material) in the first step. It then continues to react with the other components, causing a modification in their molecular structure, mainly through dehydration reactions.

Table 3 Thermostability results of the fibers

Sample	Onset degradation temperature/°C	Degradation temperature/°C	Char yield at 900 °C/wt%
UMBTF	271	302	17.08
BTF-1	297	340	20.06
BTF-2	359	399	14.04
BTF-3	345	388	13.70
BTF-4	230	278	19.20
BTF-5	–	–	50.02

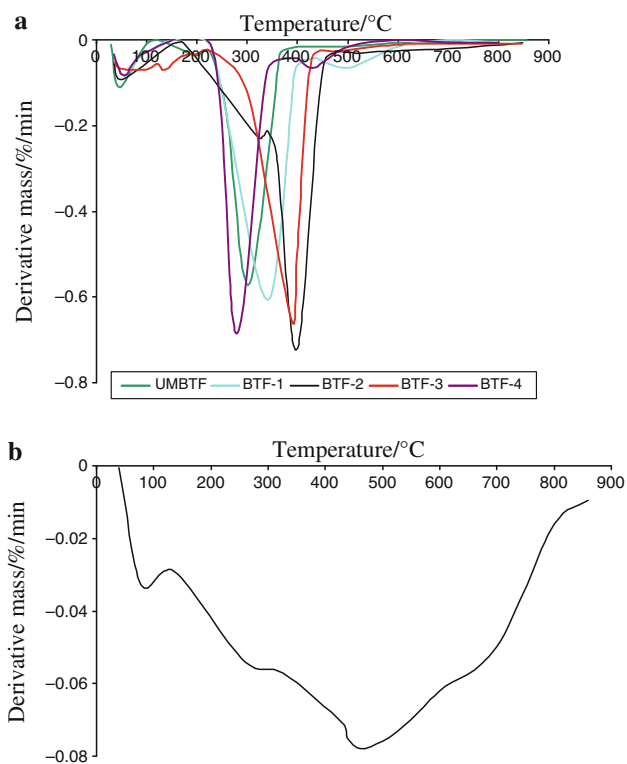


Fig. 2 Derivative thermogravimetric curve of BTF after **a** mercerization, acetylation, peroxide treatment, esterification, and **b** sulfuric acid treatment at a heating rate of 20 °C/min

Determination of apparent energy

For natural fiber reinforced polymer composite processing, it is important to understand and predict the thermal decomposition of the reinforcing fibers. The study has to be based on the simplified kinetic scheme, and the parameters under specific process temperature of polymer/natural fiber composite. The “model-free” iso-conversional approach is often employed in obtaining the activation energy. The method allows the determination of dependence on the kinetic parameters with the conversion from TG and DTG curves. These curves are measured at various heating rates without making any assumptions about the reaction order and the reaction function, thus making it impossible in

obtaining wrong kinetics parameters, especially activation energy, due to the pre-assuming inappropriate reaction function [44, 45]. This approach has been widely employed to determine the thermal degradation kinetics of some polymer/natural fiber composites [42]. ICTAC Kinetics Projects suggest that the use of single-heating rate data for the determination of kinetic parameters should be avoided, and the different kinetics analysis techniques are complementary rather than competitive [45]. Thus, the apparent activation energy should be obtained by combining the obtained results in Tables 3 and 4. The results obtained showed that the apparent activation energy of 149–210 kJ/mol was obtained for the selected fibers indicating the modifications are suitable for polymer composite processing. This range of activation energy obtained in this study, can assist in understanding the thermal decomposition stability of natural fibers used as reinforcing agents in polymer composite industry. The obtained activation energy data will be useful to the calculate thermal kinetics parameters as discussed by Malek [46].

The plots of iso-conversional Kissinger, Friedman, and F–W–O methods show a general trend of activation energy. Figure 3a represents the degradation of BTF-1 at different heating rates. Reports suggest that, to avoid compensation effects in the estimation of the kinetic constants, different heating rates should be utilized [47].

Heating rates of 5, 10, 25, 50, 7, and 100 °C were chosen to study the thermal degradation kinetics of the treated BTF fibers. A shift in the temperature of the maximum degradation rate was observed with increasing heating rate. The initial sample size of fibers was controlled to avoid the heat transfer problems at higher heating rates. This can be observed from the constant mass loss rates over the entire experimental range. From the evaluation, the major processes of degradation were considered, as indicated for the maximum temperature (DTG) in Fig. 3b. Table 4 shows the apparent activation energy values calculated using Kissinger’s method for all fibers (except BTF-5). Figure 4a shows the linear plots of $\ln(\beta/T_m^2)$ versus $1/T_m$ for various treated fibers from the Kissinger method. As an example, the Friedman plot for the BTF-2 is shown

Table 4 Average apparent activation energy of the fibers calculated Kissinger, Friedman, and Flynn–Wall–Ozawa methods

Fibers	Kissinger		Friedman*		F–W–O*	
	E_a /kJ/mol	R^2	E_a /kJ/mol	R^2	E_a /kJ/mol	R^2
UMBTF	172.40	0.9877	172.31 (13.88)	0.9900 (0.006)	175.24 (10.60)	0.9951 (0.004)
BTF-1	181.84	0.9914	178.36 (17.72)	0.9923 (0.004)	186.16 (12.94)	0.9944 (0.004)
BTF-3	152.24	0.9918	149.68 (8.24)	0.9943 (0.004)	154.34 (10.32)	0.9928 (0.004)
BTF-4	212.85	0.9931	209.76 (35.04)	0.9949 (0.003)	214.90 (33.37)	0.9969 (0.003)
BTF-5	152.24	0.9918	149.68 (8.24)	0.9943 (0.004)	154.34 (10.32)	0.9928 (0.004)

* Friedman and Flynn–Wall–Ozawa methods were calculated in a period of $\alpha = 0.2$ –0.6

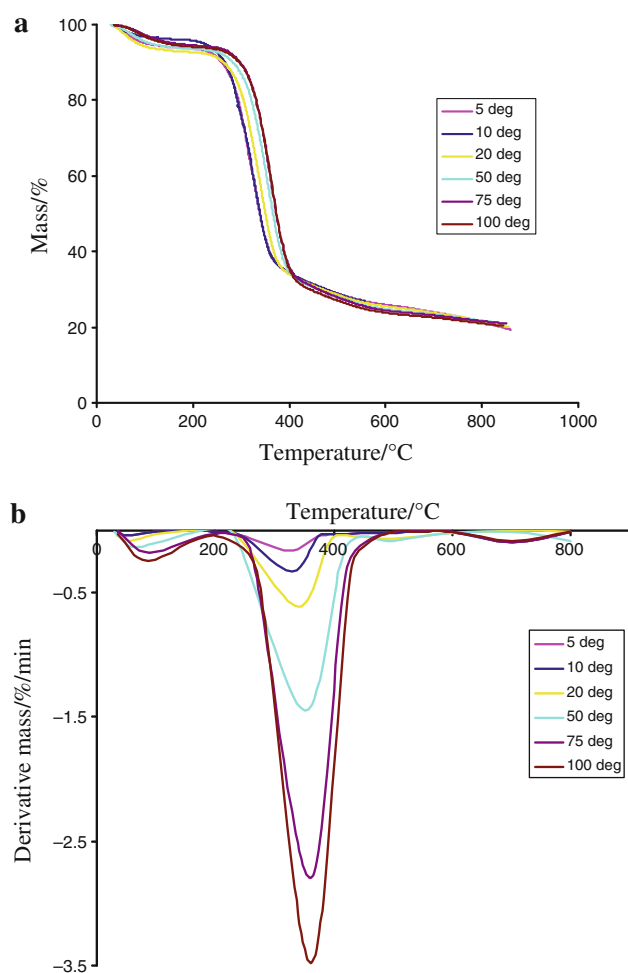


Fig. 3 a Thermogravimetric and derivative thermogravimetric curves of mercerized BTf at heating rates between 5 and 100 °C/min

in Fig. 4b, while Fig. 4c shows the specific results of application of F–W–O using BTf-3. Yao et al. [47] suggested that, high conversion periods are not recommended as the reaction mechanism might change. Hence, a conversion range of 0.2–0.6 was chosen. Table 4 summarizes the average apparent activation energies calculated from the conversion range of 0.2–0.6 through iso-conversional Friedman and F–W–O for all the treated fibers. All the data were calculated using the Excel program to accurately obtain activation energy. As shown in Table 4, the differential Friedman method led to an apparent activation energy range of approximately 149–210 kJ/mol for all the treated fibers in the conversion range. Similar results from F–W–O method were also observed confirming this conclusion. However, in the case of BTf-5 apparent energy could not be determined as mass loss occurs in a single wide step. Furthermore, the characteristic peak of maximum rate of mass loss cannot be easily distinguished.

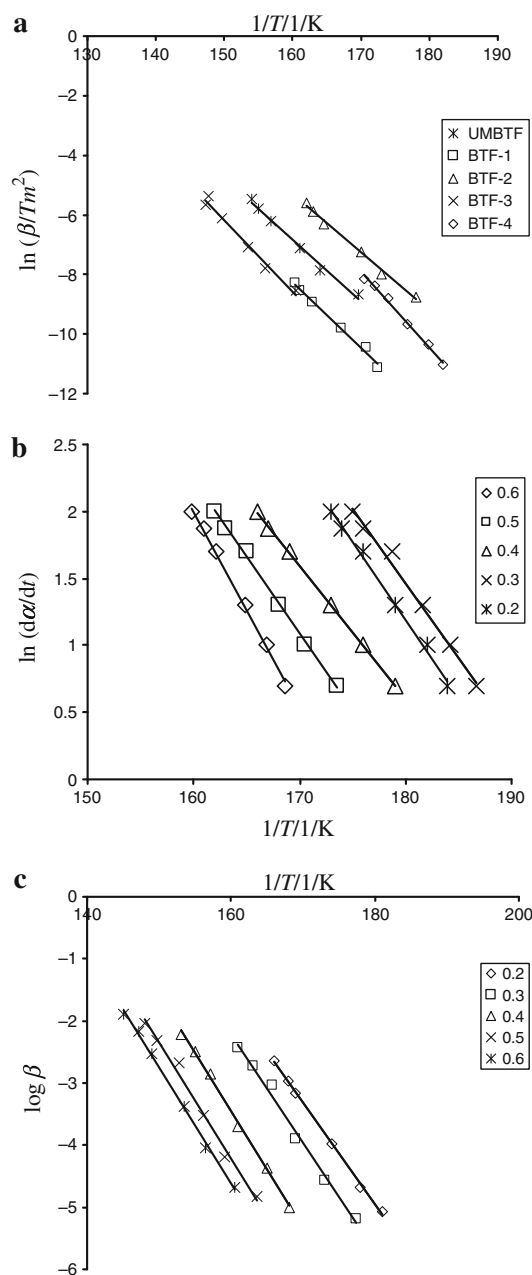
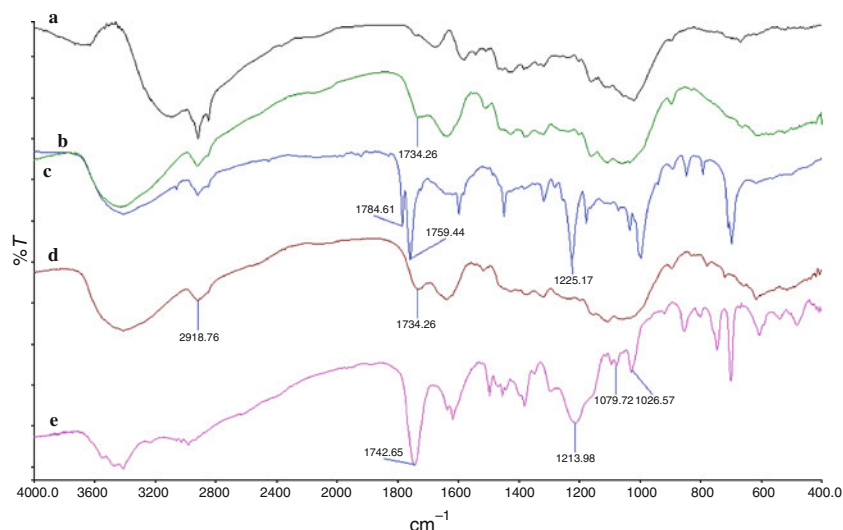


Fig. 4 Typical iso-conversional plot of a Kissinger method (all fibers), b Friedman method (acylated BTf), and c F–W–O method (peroxide treated BTf)

Infrared spectroscopy analysis

The FTIR spectra of the modified BTf are shown in Fig. 5. Identification of the most important bands is based on our previous studies of banana pseudo stem fibers [48]. In the case of BTf-1 (Fig. 5a), the vibration band at 1,250/cm which corresponds to C–O stretching in hemicellulose disappeared from alkaline treated fibers. The other noticeable changes were the band that disappeared at 1,728/cm, which attributed to the C=O stretching of methyl

Fig. 5 Plot of FTIR spectra of **a** mercerized, **b** acetylated, **c** peroxide treated, **d** esterified, and **e** sulfuric acid treated BTF



ester and carboxylic acid in hemicelluloses [40]. This indicated the removal of hemicelluloses by alkalization. The decrease in the intensity of the absorption band at 1,373 and 1,104/cm, which attributed to OH bending and C–O–H stretching of cellulose indicated that there are reactions happening between sodium ion and hydroxyl group of cellulose chain. A distinct band at around 1,734/cm was observed for BTF-2 (Fig. 5b) indicating the presence of C=O due to the ester group [49]. In BTF-3 (Fig. 5c), the peroxide treatment oxidizes the hydroxyl groups from cellulose to carboxyl groups which give the fiber a mild cationic potential [50]. This oxidation is confirmed by the bands at 1,784 and 1,759/cm. The carbonyl signal initially present is from lignin and hemicellulose; after the treatment, the formation of carboxyl groups is observed, whose axial vibration of C=O intensifies the band. An intensified band at 1,225/cm in BTF 3 was observed indicating the C–O–C axial vibration [19]. As shown in the spectra of BTF-4 (Fig. 5d) shows an absorption band at 1,734/cm indicating the presence of C=O due to esterification reaction. The prominent IR band at 2,918/cm is assigned to CH₂ asymmetric stretching vibrations, which are attributed to the hydrocarbon moiety from stearic acid. The result obtained for BTF-5 (Fig. 5e) suggests that the acid treatment causes the degradation of β -O-4 linkages, or rearrangement of other bonds that results in increased carbonyl groups (1,742/cm) within the lignin fraction [51]. Furthermore, the absorbance of the β -O-4 ether band at 1,250/cm decreased after hydrolysis. The increase in the band strength at 1,214/cm indicates an intensified contribution from second OH groups. Furthermore, the bands at 1,026 and 1,079/cm, indicate the presence of aliphatic OH groups. The results obtained indicate that the sulfuric acid treatment, cleavages the structural linkages of lignin and hemicellulose [52].

Conclusions

Dynamic TG analysis was employed to investigate the thermal decomposition of five treated BTF. The treatments are mercerization, acetylation, peroxide treatment, esterification, and sulphonation. The common iso-conventional methods (Kissinger, Friedman, and Flynn–Wall–Ozawa) were employed to determine the apparent activation energy of these fibers. A similar degradation pattern was observed for all the treated BTF (except for BTF-5), as the base material is cellulosic fibers. The obtained curves had distinct peak and a high temperature tail which is attributed to cellulose and lignin, respectively. Decomposition temperature of the treated fibers increased in the order of esterification > untreated > mercerization > peroxide treated > acetylation. The apparent activation energy of the treated fibers is within the polymer processing temperature range, indicating that the modification is suitable for polymer composite processing.

Acknowledgements This study is partially funded by the Ministry of Science, Technology, and Innovation (MOSTI) of Malaysia. The authors are also grateful to the School of Chemical Sciences, Universiti Sains Malaysia, and the Faculty of Applied Sciences, AIMST University for providing the facilities to carry out this research.

References

- Zena S, Ng L, Simon C, Elkamel A. Renewable agricultural fibers as reinforcing fillers in plastics prediction of thermal properties. *J Therm Anal Calorim.* 2009;96:85–90.
- Li Y, Mai YW, Ye L. Sisal fibers and its composites; a review of recent developments. *Compos Sci Technol.* 2000;60:2037–55.
- Kumar S, Choudhary V, Kumar R. Study on the compatibility of unbleached and bleached bamboo-fiber with LLDPE matrix. *J Therm Anal Calorim.* 2010;102:751–61.

4. Mohd Edeerozey AM, Md Akil H, Azhar AB, Zainal AMI. Chemical modification of kenaf fibers. *Mater Lett.* 2007;61:2020–5.
5. John MJ, Thomas S. Biofibers and biocomposites review. *Carbohydr Polym.* 2008;71:343–64.
6. Sreekala MS, Thomas S, Neelakantan NR. Utilization of short oil palm fiber bunch fruit (OPEFB) as a reinforcement in phenol-formaldehyde resins: studies on mechanical properties. *J Polym Eng.* 1997;16:265–94.
7. Selzer R, Friedrich K. Influence of water-up-take on interlaminar fracture properties. Influence of water up-take on interlaminar fracture properties of carbon fiber-reinforced polymer composites. *J Mater Sci.* 1995;30:334–8.
8. Rana AK, Manda A, Mitra BC, Jacobson R, Rowell R, Banerjee AN. Short jute fiber-reinforced polypropylene composites: effect of compatibilizer. *J Appl Polym Sci.* 1997;69:329–38.
9. Goda K, Sreekala MS, Gomes A, Kaji T, Ohgi J. Improvement of plant based natural fibers for toughening green composites-effect of load application during mercerization of ramie fibers. *Compos A.* 2006;37:2213–20.
10. Cantero G, Arbelaz A, Llano-Ponte R, Mondragon I. Effects of fiber treatment on wettability and mechanical behavior of flax/polypropylene composites. *Compos Sci Technol.* 2003;60:1247–54.
11. Awal A, Ghosh SB, Sain M. Thermal properties and spectral characterization of wood pulp reinforced bio-composite fibers. *J Therm Anal Calorim.* 2010;99:695–701.
12. Li X, Tabil LG, Panigrahi S. Chemical treatments of natural fiber for use in natural fiber-reinforced composites: a review. *J Polym Environ.* 2007;15:25–33.
13. Ray D, Sarkar BK, Rana AK, Bose NR. Effect of alkali treated jute fibers on composite properties. *Bull Mater Sci.* 2001;24:129–35.
14. Mishra S, Misra M, Tripathy SS, Nayak SK, Mohanty AK. Graft copolymerization of acrylonitrile on chemically modified sisal fibers. *Macromol Mater Eng.* 2001;286:107–13.
15. Van de Weyenberg I, Ivens J, De Coster A, Kino B, Baetens E, Vepoes I. Influence of processing and chemical treatment of flax fibers on their composites. *Compos Sci Technol.* 2003;63:1241–6.
16. Saheb DN, Jog JP. Natural fiber polymer composites: a review. *Adv Polym Technol.* 1999;18:351–5.
17. Maya J, Bejoy F, Sabu T, Varughese KT. Dynamical mechanical analysis of sisal/oil palm hybrid fiber-reinforced natural rubber composites. *Polym Compos.* 2006;27:671–80.
18. Guimarães JL, Frollini E, da Silva CG, Wypych F, Satyanarayana KG. Characterization of banana, sugarcane bagasse and sponge gourd fibers of Brazil. *Ind Crop Prod.* 2009;30:407–15.
19. Bilba K, Arsene MA, Ouensanga A. Study of banana and coconut fibers; botanical composition, thermal degradation and textural observations. *Bioresour Technol.* 2007;98:8–68.
20. Nolasco AM, Soffner MLAP, Nolasco AC. Physical-mechanical characterization of banana fiber, *Musa cavendish*-nanicao variety. In: Mattoso LHC, Leão AL, Frollini E, editors. Second international symposium on natural polymers and composites. Sao Carlos: Embrapa Agricultural Instrumentation, São Paulo University (USP), São Paulo State University (UNESP); 1998.
21. Satyanarayana KG, Wypych F. Characterization of natural fibers. In: Fakirov S, Bhattacharya D, editors. *Engineering biopolymers: homopolymers, blends and composites.* Munich: Hanser Publishers; 2007.
22. Kulkarni AG, Satyanarayana KG, Rohatgi PK. Mechanical properties of banana fibers (*Musa Sepientum*). *J Mater Sci.* 1983;18:2290–6.
23. Idicula M, Malhotra SK, Joseph K, Thomas S. Dynamic mechanical analysis of randomly oriented intimately mixed short banana/sisal hybrid fiber reinforced polyester composites. *Compos Sci Technol.* 2005;65:1077–87.
24. Pothan LA, Thomas S, Groeninckx G. The role of fiber/matrix interactions on the dynamic mechanical properties of chemically modified banana fiber/polyester composites. *Compos A.* 2006;27:1260–9.
25. Sapuan SM, Leenie A, Harimi M, Beng YK. Mechanical properties of woven banana fiber reinforced epoxy composites. *Mater Des.* 2006;27:689–93.
26. Kalia S, Kaith BS, Kaur I. Pretreatments of natural fibers and their application as reinforcing material in polymer composites—a review. *Polym Eng Sci.* 2009;49:1253–72.
27. Kissinger HE. Variation of peak temperature with heating rate in differential thermal analysis. *J Res Natl Bur Stand.* 1956;57:217–21.
28. Friedman HL. Kinetics of thermal degradation of char-forming plastics from thermogravimetry, application of a phenolic plastic. *J Polym Sci C.* 1964;6:183–95.
29. Flynn JH, Wall LA. General treatment of thermogravimetry of polymers. *J Res Natl Bur Stand A.* 1966;70:487–523.
30. Ozawa T. A new method of analyzing thermogravimetric data. *Bull Chem Soc Jpn.* 1965;38:1881–6.
31. Horsfall M, Spiff AI. Effects of temperature on the sorption of Pb^{2+} and Cd^{2+} from aqueous solution by *Caladium bicolor* (wild cocoyam) biomass. *Electron J Biotechnol.* 2004;7:313–23.
32. Sreekala MS, Thomas S. Effect of fiber surface modification on water sorption characteristics of oil palm fibers. *Compos Sci Technol.* 2003;53:861–9.
33. Paul A, Joseph K, Thomas S. Effect of surface treatment on the electrical properties of low-density polyethylene composites reinforced with short sisal fibers. *Compos Sci Technol.* 1997;57:67–79.
34. Banerjee SS, Joshi MV, Jayaram RV. Treatment of oil spill by sorption technique using fatty acid grafted sawdust. *Chemosphere.* 2006;64:1026–31.
35. Azhar SS, Liew GA, Suhardy D, Farizul K, Hatim MD. Dye removal from aqueous solution by using adsorption on treated sugarcane bagasse. *Am J Appl Sci.* 2005;2:1499–503.
36. Yang H, Yan R, Chen H, Lee DH, Zheng C. Characteristics of hemicellulose, cellulose and lignin pyrolysis. *Fuel.* 2007;86:1781–8.
37. Antal MJ, Varhegyi G. Cellulose pyrolysis kinetics the current state knowledge. *Ind Eng Chem Res.* 1995;34:703–17.
38. Corradini E, Teixeira M, Paladin PD, Agnelli JA, Silva ORRF, Mattoso LHC. Thermal stability and degradation kinetic study of white and colored cotton fibers by thermogravimetric analysis. *J Therm Anal Calorim.* 2009;2:415–9.
39. Yang HP, Yan R, Chen HP, Zheng CG, Lee DH, Liang DT. Mechanism of palm oil wastes pyrolysis in a packed bed. *Energy Fuels.* 2006;20:1120–8.
40. Ouajai S, Shanks RA. Composition, structure and thermal degradation of hemp cellulose after chemical treatments. *Polym Degrad Stab.* 2005;89:327–35.
41. Jandura P, Riedl B, Kokta BV. Thermal degradation behavior of cellulose fibers partially esterified with some long chain organic acids. *Polym Degrad Stab.* 2000;70:387–94.
42. Alvarez P, Blanco C, Santamaria R, Granda M. Improvement of the thermal stability of lignocellulosic materials by treatment with sulfuric acid and potassium hydroxide. *J Anal Appl Pyrolysis.* 2004;72:131–9.
43. Vollhardt KPC. *Organic chemistry.* New York: Freeman; 1987.
44. Maciejewski M. Computational aspects of kinetic analysis, part B: The ICTAC kinetics project—the decomposition kinetics of calcium carbonate revisited, or some tips on survival in the kinetic minefield. *Thermochim Acta.* 2000;355:145–54.
45. Brown ME, Maciejewski M, Vyazovkin S, Nomen R, Sempere J, Burnham A, Opfermann J, Strey R, Anderson HL, Kemmler A, Keuleers R, Janssens J, Desseyn HO, Li CR, Tang TB, Roduit B,

- Malek J, Mitsunashi T. Computational aspects of kinetic analysis, part A: The ICTAC kinetics, project: data, methods, and results. *Thermochim Acta Spec.* 2000;355:125–43.
46. Malek J. The kinetic-analysis of nonisothermal data. *Thermochim Acta.* 1992;200:257–69.
47. Yao F, Wu Q, Lei Y, Guo W, Xu Y. Thermal decomposition kinetics of natural fibers: activation energy with dynamic thermogravimetric analysis. *Polym Degrad Stab.* 2008;93:90–8.
48. Mas Haris MRH, Kathiresan S. The removal of methyl red from aqueous solutions using banana pseudostem fibers. *Am J Appl Sci.* 2009;6:1690–700.
49. Sen AK, Kumar S. Coir-fiber-based fire retardant nano filler for epoxy composites. *J Therm Anal Calorim.* 2010;101:265–71.
50. Brígida AIS, Calado VMA, Gonçalves LRB, Coelho MAZ. Effect of chemical treatments on properties of green coconut fiber. *Carbohydr Polym.* 2010;79:32–838.
51. Sun XF, Xu F, Sun RC, Wang YX, Fowler P, Baird MS. Characteristics of degraded lignins obtained from steam exploded wheat straw. *Polym Degrad Stab.* 2004;86:45–256.
52. Grabber JH. How do lignin composition, structure, and cross-linking affect degradability? A review of cell wall model studies. *Crop Sci.* 2005;45:820–31.